Hemodynamic responses to antivascular therapy and ionizing radiation assessed by diffuse optical spectroscopies

Ulas Sunar[1], Sosina Makonnen[†], Chao Zhou, Turgut Durduran[‡], Guoqiang Yu, Hsing-Wen Wang, William M. F. Lee[†] and Arjun G. Yodh

[1]*Dept. of Radiology, University of California San Diego, CA, 92093*
Dept. of Physics and Astronomy, University of Pennsylvania, Philadelphia, PA, 19104
[‡]*Dept. of Radiology and Dept. of Physics and Astronomy, University of Pennsylvania, PA, 19104*
[†]*Dept. of Medicine and the Abramson Cancer Center, University of Pennsylvania, Philadelphia, PA, 19104*
sunar@sas.upenn.edu

Abstract: Diffuse optical methods were used to monitor two different therapies in K1735 malignant mouse melanoma tumor models: anti-vascular therapy and radiation therapy. Anti-vascular therapy induced acute variation in hemodynamic parameters within an hour, and radiation therapy induced longitudinal changes within 2 weeks. During anti-vascular therapy, the drug Combretastatin A-4 3-O-Phosphate (CA4P, 2.5 mg/200 μl PBS/mouse) significantly decreased tissue blood flow (65%) and blood oxygenation (38%) one hour after injection. In the longitudinal study, single-fraction ionizing radiation (12 Gy x 1) induced significant reduction of tissue blood flow (36%) and blood oxygenation (24%) 14 days after radiation. The results correlated well with contrast enhanced ultrasound, tumor histology, and a nitroimidazole hypoxia marker (EF5). The research provides further evidence that noninvasive diffuse optical spectroscopies can be useful tools for monitoring cancer therapy *in vivo*.

OCIS codes: (170.0110) Imaging systems; (170.3660) Light propagation in tissues; (170.3880) Medical and biological imaging; (170.6480) Spectroscopy, speckle.

References and links

1. P. Vaupel, F. Kallinowski, and P. Okunieff. "Blood flow, oxygen and nutrient supply, and metabolic microenvironment of human tumors: A review," Cancer Res. **49**, 6449–6465 (1989).
2. R. K. Jain. "Normalizing tumor vasculature with anti-angiogenic therapy: a new paradigm for combination therapy," Nat. Med. **7**, 987–989 (2001).
3. R. K. Jain, L. L. Munn, and D. Fukumura. "Dissecting tumour pathophysiology using intravital microscopy," Nat. Rev. Cancer **2**, 266–276 (2002).
4. D.M. Brizel, G.S. Sibley, L.R. Prosnitz, R.L. Scher, and M.W. Dewhirst. "Tumor hypoxia adversely affects the prognosis of carcinoma of the head and neck," Int. J. Radiat. Oncol. Biol. Phys. **38**, 285–289 (1997).
5. M. Nordsmark, S.M. Bentzen, and J. Overgaard. "Pretreatment oxygenation predicts radiation response in advanced squamous cell carcinoma of the head & neck," Radiother. Oncol. **41**, 31–39 (1996).
6. L.H. Gray, A.D. Conger, M. Ebert, S. Horsney, and O.C.A. Scott. "The concentration of oxygen dissolved in tissue at the time of irradiation as a factor in radiotherapy," Br. J. Radiol. **26**, 638–42 (1953).
7. R.F. Kallman. "The phenomenon of reoxygenation and its implications for fractionated radiotherapy," Radiol. **105**, 135–142 (1972).

#87255 - $15.00 USD Received 6 Sep 2007; revised 26 Oct 2007; accepted 29 Oct 2007; published 8 Nov 2007

8. A. F. DeVries, C. Kremser, P. A. Hein, J. Griebel, A. Krezcy, D. Ofner, K. P. Pfeiffer, P. Lukas, and W. Judmaier. "Tumor microcirculation and diffusion predict therapy outcome for primary rectal carcinoma," Int. J. Radiat. Oncol. Biol. Phys. **56**, 958–965 (2003).
9. N. A. Mayr, W. T. Yuh, V. A. Magnotta, J. C. Ehrhardt, J. A. Wheeler, J. I. Sorosky, C. S. Davis, B. C. Wen, D. D. Martin, R. E. Pelsang, R. E. Buller, L. W. Oberley, D. E. Mellenberg, and D. H. Hussey. "Tumor perfusion studies using fast magnetic resonance imaging technique in advanced cervical cancer: a new noninvasive predictive assay," Int. J. Radiat. Oncol. Biol. Phys. **36**, 623–633 (1996).
10. D.W. Siemann, K.H. Warrington, and M.R. Horsman. "Ionizing radiation inhibits tumor neovascularization by inducing ineffective angiogenesis," Radiother. Oncol. **57**, 5–12 (2000).
11. R. Murata, D. W. Siemann, J. Overgaard, and M. R. Horsman. "Improved tumor response by combining radiation and the vascular-damaging drug 5,6-dimethylxanthenone-4-acetic acid," Radiat. Res. **156**, 503–509 (2001).
12. R. Murata, D. W. Siemann, J. Overgaard, and M. R. Horsman. "Interaction between combretastatin A-4 disodium phosphate and radiation in murine tumors," Radiother. Oncol. **60**, 155–161 (2001).
13. A. G. Yodh and D. A. Boas, *Biomedical Photonics* (CRC Press, 2003). Chapter Functional Imaging with Diffusing Light.
14. C. Cheung, J. P. Culver, K. Takahashi, J. H. Greenberg, and A. G. Yodh. "In vivo cerebrovascular measurement combining diffuse near-infrared absorption and correlation spectroscopies," Phys. Med. Biol. **46**, 2053–2065 (2001).
15. J. P. Culver, T. Durduran, D. Furuya, C. Cheung, J. H. Greenberg, and A. G. Yodh. "Diffuse optical tomography of cerebral blood flow, oxygenation, and metabolism in rat during focal ischemia," J. Cereb. Blood Flow Metab. **23**, 911–924 (2003).
16. C. Zhou, G. Yu, F. Daisuke, J. H. Greenberg, A. G. Yodh, and T. Durduran. "Diffuse optical correlation tomography of cerebral blood flow during cortical spreading depression in rat brain," Opt. Express **14**, 1125–1144 (2006).
17. T. Durduran, G. Yu, M. G. Burnett, J. A. Detre, J. H. Greenberg, J. Wang, C. Zhou, and A. G. Yodh. "Diffuse optical measurement of blood flow, blood oxygenation, and metabolism in a human brain during sensorimotor cortex activation," Opt. Lett. **29**, 1766–1768 (2004).
18. J. Li, G. Dietsche, D. Iftime, S. E. Skipetrov, G. Maret, T. Elbert, B. Rockstroh, and T. Gisler. "Noninvasive detection of functional brain activity with near-infrared diffusing-wave spectroscopy," J. Biomed. Opt. **10**, 44002 (2005).
19. G. Yu, T. Durduran, G. Lech, C. Zhou, B. Chance, E. R. Mohler III, and A. G. Yodh. "Time-dependent blood flow and oxygenation in human skeletal muscle measured by noninvasive near-infrared diffuse optical spectroscopies," J. Biomed. Opt. **10**, 024027 (2005).
20. U. Sunar, H. Quon, T. Durduran, J. Zhang, J. Du, C. Zhou, G. Yu, R. Choe, A. Kilger, R. Lustig, L. Loevner, S. Nioka, B. Chance, and A.G. Yodh. "Noninvasive diffuse optical measurement of blood flow and blood oxygenation for monitoring radiation therapy in patients with head and neck tumors," J. Biomed. Opt. **11**, 064021 (2006).
21. T. Durduran, R. Choe, G. Yu, C. Zhou, J. C. Tchou, B. J. Czerniecki, and A. G. Yodh. "Diffuse optical measurement of blood flow in breast tumors," Opt. Lett. **30**, 2915–2917 (2005).
22. C. Zhou, R. Choe, N. Shah, T. Durduran, G. Q. Yu, A. Durkin, A. Cerussi, D. Hsiang, R. Mehta, B. J. Tromberg, and A. G. Yodh. "Diffuse optical monitoring of blood flow and oxygenation in human breast cancer during early stages of neoadjuvant chemotherapy," J. Biomed. Opt. **12**, 051903 (2007).
23. G. Yu, T. Durduran, H. W. Wang, C. Zhou, H. M. Saunders, C. M. Sehgal, T. M. Busch, and A. G. Yodh. "Noninvasive monitoring of hemodynamic responses in RIF tumors during and after PDT," Clin. Cancer Res. **11**, 3543–3552 (2005).
24. Turgut Durduran, "Noninvasive measurements of tissue hemodynamics with hybrid diffuse optical methods," Ph.D. Thesis, University of Pennsylvania (2004).
25. G. Yu, T. F. Floyd, T. Durduran, C. Zhou, J. J. Wang, J. A. Detre, and A. G. Yodh. "Validation of diffuse correlation spectroscopy for muscle blood flow with concurrent arterial spin labeled perfusion MRI," Opt. Express **15**, 1064–1075 (2007).
26. R. Choe, A. Corlu, K. Lee, T. Durduran, S. D. Konecky, M. Koptyra, S. R. Arridge, B. J. Czerniecki, D. L. Fraker, A. DeMichele, B. Chance, M. Rosen, and A. G. Yodh. "Diffuse optical tomography of breast cancer during neoadjuvant chemotherapy: A case study with comparison to MRI," Med. Phys. **32**, 1–11 (2005).
27. Q. Zhu, S. H. Kurtzmany, P. Hegde, S. Tannenbaum, M. Kane, M. Huang, N. G. Chen, B. Jagjivan, and K. Zarfos. "Utilizing optical tomography with ultrasound localization to image heterogeneous hemoglobin distribution in large breast cancers," Neoplasia **7**, 263–270 (2005).
28. D. B. Jakubowski, A. E. Cerussi, F. Bevilacqua, N. Shah, D. Hsiang, J. Butler, and B. J. Tromberg. "Monitoring neoadjuvant chemotherapy in breast cancer using quantitative diffuse optical spectroscopy: A case study," J. Biomed. Opt. **9**, 230–238 (2004).
29. L. S. Ziemer, W. M. F. Lee, S. A. Vinogradov, C. Sehgal, and D. F. Wilson. "Oxygen distribution in murine tumors: characterization using oxygen-dependent quenching of phosphorence," J. Appl. Physiol. **98**, 1503–1510 (2005).

#87255 - $15.00 USD Received 6 Sep 2007; revised 26 Oct 2007; accepted 29 Oct 2007; published 8 Nov 2007

30. C. M. Sehgal, P. H. Arger, S. E. Rowling, E. F. Conant, C. Reynolds, and J. A. Patton. "Quantitative vascularity of breast masses by Doppler imaging: Regional variations and diagnostic implications," J. Ultrasound Med. **19**, 427–440 (2000).
31. S. M. Evans, S. Hahn, D. R. Pook, W. T. Jenkins, A. A Chalian, P. Zhang, C. Stevens, R. Weber, G. Weinstein, I. Benjamin, N. Mirza, M. Morgan, S. Rubin, W. G. McKenna, E. M. Lord, and C. J. Koch. "Detection of hypoxia in human squamous cell carcinoma by EF5 binding," Cancer Res. **60**, 2018–2024 (2000).
32. G. Maret and P. E. Wolf. "Multiple light scattering from disordered media. the effect of brownian motion of scatterers," Z. Phys. B **65**, 409–413 (1987).
33. D. J. Pine, D. A. Weitz, P. M. Chaikin, and E. Herbolzheimer. "Diffusing wave spectroscopy," Phys. Rev. Lett. **60**, 1134–1137 (1988).
34. D. A. Boas, L. E. Campbell, and A. G. Yodh. "Scattering and imaging with diffusing temporal field correlations," Phys. Rev. Lett. **75**, 1855–58 (1995).
35. M. Heckmeier, S. E. Skipetrov, G. Maret, and R. Maynard. "Imaging of dynamic heterogeneities in multiple-scattering media," J. Opt. Soc. Am. A **14**, 185–191 (1997).
36. Chao Zhou, "In vivo optical imaging and spectroscopy of cerebral hemodynamics," Ph.D. Thesis, University of Pennsylvania (2007).
37. B. J. Berne and R. Pecora. "Dynamic Light Scattering," (1976) (New York,Wiley).
38. D. A. Boas and A. G. Yodh. "Spatially varying dynamical properties of turbid media probed with diffusing temporal light correlation," J. Opt. Soc. Am. A **14**, 192–215 (1997).
39. B. C. Wilson, T. J. Farrell, and M. S. Patterson. "An optical fiber-based diffuse reflectance spectrometer for non-invasive investigation of photodynamic sensitizers in vivo," Proc. SPIE **6**, 219–232 (1990).
40. H. W. Wang, M. E. Putt, M. J. Emanuele, D. B. Shin, E. Glatstein, A. G. Yodh, and T. M. Busch. "Treatment-induced changes in tumor oxygenation predict photodynamic therapy outcome," Cancer Res. **64**, 7553–7561 (2004).
41. H. W. Wang, T. C. Zhu, M. E. Putt, M. Solonenko, J. Metz, A. Dimofte, J. Miles, D. L. Fraker, E. Glatstein, S. M. Hahn, and A. G. Yodh. "Broadband reflectance measurement of light penetration, blood oxygenation, hemoglobin concentration, and drug concentration in human intraperitoneal tissues before and after photodynamic therapy," J. Biomed. Opt. **10**, 014004 (2005).
42. S. Prahl. "Optical properties spectra (webpage http://omlc.ogi.edu/spectra/index.html)," (2001).
43. J.H. Tsai, S. Makonnen, M. Feldman, C.M. Sehgal, A. Maity, and W.M. Lee. "Ionizing radiation inhibits tumor neovascularization by inducing ineffective angiogenesis," Cancer Biol. Ther. **4**, 1395–1400 (2005).
44. M. Kragh, B. Quistorff, M. R. Horsman, and P. E. G. Kristjansen. "Acute effects of vascular modifying agents in solid tumors assessed by noninvasive laser Doppler flowmetry and near infrared spectroscopy," Neoplasia **4**, 263–267 (2002).
45. D. A. Beauregard, P. E. Thelwall, D. J. Chaplin, S. A. Hill, G. E. Adams, and K. M. Brindle. "Magnetic resonance imaging and spectroscopy of combretastatin A4 prodrug-induced disruption of tumour perfusion and energetic status," Br. J. Cancer **77**, 1761–1767 (1998).
46. D. E. Goertz, J. L. Yu, R. S. Kerbel, P. N. Burns, and F. S. Foster. "High-frequency Doppler ultrasound monitors the effects of antivascular therapy on tumor blood flow," Cancer Res. **62**, 6371–6375 (2002).
47. S. M. Galbraith, R. J. Maxwell, M. A. Lodge, G. M. Tozer, J. Wilson, N. J. Taylor, J. J. Stirling, L. Sena, A. R. Padhani, and G. J. S. Rustin. "Combretastatin A4 phosphate has tumor antivascular activity in rat and man as demonstrated by dynamic magnetic resonance imaging," J. Clin. Oncol. **21**, 2831–2842 (2003).
48. G. M. Tozer. "Measuring tumour vascular response to antivascular and antiangiogenic drugs," Br. J. Radiol. **76**, 23–35 (2003).
49. H. L. Anderson, J. T. Yap, M. P. Miller, A. Robbins, T. Jones and P. M. Price. "Assessment of pharmacodynamic vascular response in a phase I trial of Combretastatin A4 Phosphate," J. Clin. Oncol. **21**, 2823–2830 (2003).

1. Introduction

Knowledge of tumor hemodynamic properties such as blood oxygenation and blood flow can inform tumor therapy and permit optimization of individual treatment protocols [1–3]. Thus noninvasive, repetitive measurements of these parameters are attractive in the clinical context. Radiation, for example, is an important nonsurgical tool for treatment of tumors for which tumor oxygen status affects therapy outcome [4, 5]; in this case higher radiation doses are needed to kill hypoxic tumor cells compared to well-oxygenated cells [1, 6, 7]. In a different vein, tumor responses to drug therapies depend on adequate blood flow to replenish tissue oxygen and for efficient drug delivery [8, 9]; in some cases anti-vascular drug therapy has even been used as an adjuvant strategy for radiation therapy, enhancing radiation efficacy by modifying tumor vasculature and consequently, tumor blood flow and oxygenation [10–12].

#87255 - $15.00 USD Received 6 Sep 2007; revised 26 Oct 2007; accepted 29 Oct 2007; published 8 Nov 2007

Repetitive measurements of blood flow and oxygenation are also valuable for pre-clinical animal studies that, for example, facilitate further understanding of antivascular agents and their translation to the clinic. In this study we focus on the potential of diffuse optics for frequent assessment of tissue hemodynamics in pre-clinical models. In particular, we investigate tumor blood flow and blood oxygenation changes induced by an anti-vascular drug, Combretastatin A-4 3-O-Phosphate (CA4P), and by radiation. We employ two noninvasive optical methods for these studies: diffuse correlation spectroscopy (DCS) and diffuse reflectance spectroscopy (DRS).

Diffuse correlation spectroscopy (DCS) measures the temporal fluctuations of light transmitted through tissue and enables us to assess dynamical changes of tumor blood flow by detecting the motion of blood cells. To date DCS has been successfully employed in animal studies [13–16], in human brain [17, 18], in muscle [19], and for head and neck [20] and breast [21, 22] tumor monitoring. Validation of DCS in some cases has been provided by comparison to power Doppler ultrasound [23], laser Doppler [24] and arterial spin labeled MRI [25]. Diffuse reflectance spectroscopy (DRS) is a more traditional near-infrared (NIR) spectroscopy approach that uses the average attenuation and phase shift of scattered light to derive information about blood oxygen saturation; it has recently been applied in therapy monitoring [20, 26–28].

Herein we report on measurements of hemodynamics induced by CA4P and by the radiation in K1735 malignant melanoma tumor models. Our results clearly demonstrate CA4P induced rapid shutdown of tumor blood flow and tumor hypoxia. On the other hand, radiation effects were delayed; significant reductions in both blood flow and oxygenation occurred during the second week. The research further validates and corroborates the utility of the diffuse optical methodologies in a useful context.

2. Methods

2.1. Animal and tumor model

All animal experiments were approved by the University of Pennsylvania Animal Care and Use Committee. Six- to 8-week-old C3H/HeN female mice were purchased from Harlan Sprague Dawley (Indianapolis, IN) and were maintained in micro-isolator cages under sterile conditions. The K1735 melanoma tumor cell lines were cultured and injected subcutaneously into anesthetized mice. Measurements were made when tumors reached a diameter of 6-10 mm, generally 2-3 weeks after cell inoculation. During diffuse optical measurements mice were anesthetized with an isoflurane and air mixture.

For antivascular therapy study, 9 and 5 mice were used for DCS and DRS measurements, respectively. Optical measurements were carried out $\sim$5 minutes before CA4P injection to provide a baseline and after 1 hour to provide post injection information. DCS was continuously employed during the 1 hour period. At least 2 repeated measurements were obtained for DCS and 10 repeated measurements were carried out for DRS. For radiation therapy experiments, the first group of mice were irradiated using a Philips X-ray generator operating at 225 kV, 17 mA, and using a 0.2 μm Cu filter at a dose rate of 3.4 Gy/min. The mice bodies were shielded with lead except for the tumor-bearing hind limb. Tumors were irradiated with 12 Gy in a single fraction ($N = 8$). Optical measurements were carried out prior to radiation to provide a baseline, and then were carried out again at 7-days and 14-days post-radiation. Control tumors ($N = 8$), which did not receive radiation and grew more quickly than the radiated ones, were measured at baseline, 5-days and 12-days after baseline measurements. Minimum 5 repeated measurements were carried out for each group by positioning the optical probe on different tumor locations. Therefore, the averages presented in this paper represent the mean obtained from a total of $(N_{animals}) \times (N_{repeated\ measurements})$ data sets for both studies.

#87255 - $15.00 USD Received 6 Sep 2007; revised 26 Oct 2007; accepted 29 Oct 2007; published 8 Nov 2007

2.2. Contrast-enhanced ultrasound imaging

To corroborate the optical blood flow measurements, representative tumors ($N = 2$) in each group were also imaged using contrast-enhanced Doppler ultrasound with a Philips ATL 5000 ultrasound scanner (Philips ATL, Bothell, WA) [23, 29]. The ultrasound measurements were carried out just prior to the optical measurements. Initial scanning of each tumor was performed in grayscale ultrasound mode to define the boundary of the tumor mass. Mice were then injected with one hundred micro-liters of micro-bubble ultrasound contrast agent (Optison, Amersham, Princeton, NJ) via tail vein catheter. The area of contrast enhancement denoted perfused regions in the tumor. Tissue regions with blood flow are color coded [30].

2.3. Tumor histology and immunohistochemistry

Tumor histology analysis were performed using Hematoxylin and Eosin (H&E) staining. All histological tumor section specimens were viewed under a Nikon E600 Eclipse (Nikon, Melville, NY) equipped with a krypton-argon laser and optical filters for visualization of the dyes FITC (fluorescein isothiocyanate), Texas-red and cyanine-3 by fluorescence. Images were acquired by a charged-coupled device (CCD) camera (Roper Scientific, Trenton, NJ). Nitroimidazole (EF5) staining was performed 5 hours post-CA4P injection to determine tumor cell hypoxia. Immunofluorescent analysis of EF5 in tumor sections were performed as previously described [29, 31], using a cyanine 3-conjugated anti-EF5 monoclonal antibody. In the case of intracellular hypoxia, EF5 binding occurs and hypoxic tumor cells stain reddish.

2.4. Diffuse optical spectroscopies

DCS was used to monitor blood flow. The details of the DCS method and further background information can be found elsewhere [14, 32–36]. Briefly, the electric field temporal autocorrelation function of the scattered light depends on the motion of the red blood cells. Diffusing photons that scatter from moving blood cells experience phase shifts which cause the intensity of the diffusing light to fluctuate in time. The fluctuations are more rapid for faster moving blood cells, or for tissues with greater numbers of moving blood cells. To insure deeper penetration, the DCS light source wavelength is typically chosen in the near-infrared range. Therefore, one can derive information about deep tissue blood flow from measurements of temporal fluctuations impressed upon the transmitted near-infrared light [34].

Our custom built DCS instrument consists of a long coherence length (> 50 m) laser (Crysta Laser, Nevada) operating at 785 nm, an optical switch (Dicon Fiberoptics, California), single photon-counting fast avalanche photodiodes (Perkin-Elmer, Canada), and a non-contact probe [23] wherein source and detector fibers were located in the image plane of a regular SLR camera, permitting continuous non-contact measurements with source-detector separations ranging from 1 to 4 mm. Photodetector outputs are fed into a correlator board (Correlator.com, New Jersey) that computes light intensity temporal autocorrelation functions that are recorded by a computer [24].

From light intensity temporal autocorrelation functions, one readily extracts the data needed to derive normalized electric field ($E(r,t)$) autocorrelation function, $g_1(r,\tau) = G_1(r,\tau)/ < E^*(r,t)E(r,t) >$, where $G_1(r,\tau) =< E(r,t)E^*(r,t+\tau) >$ is the electric field autocorrelation function [37]. It has been shown that $G_1(r,\tau)$ satisfies the correlation diffusion equation in highly scattering media [34, 35, 38] and it has been shown empirically in several physiological settings that the extracted parameters αD_B characterize the temporal fluctuations of the medium due to scatterer motions such as blood flow [14, 15, 18, 25]. Here α is a factor representing the probability that a scattering event in tissue is from a moving scatterer (α is generally proportional to tissue blood volume fraction) and D_B is an "effective" diffusion coefficient for the blood cells. In this paper we report relative blood flow, rBF, to describe blood

#87255 - $15.00 USD Received 6 Sep 2007; revised 26 Oct 2007; accepted 29 Oct 2007; published 8 Nov 2007

flow changes: rBF is a blood flow parameter measured relative to its pre-treatment value, i.e. $rBF = \alpha D_B/(\alpha D_B)_{baseline}$, where the baseline value ($(\alpha D_B)_{baseline}$) was obtained in a fashion similar to the other time points.

Noninvasive tissue oxygen saturation is assessed using a broadband diffuse reflectance spectrometer. The original design principle of our *in vivo* spectrometer is due to Wilson [39]; it consists of a tungsten halogen lamp (Cuda Fiberoptics), dispersion system (monochromator, Acton Reseach), and liquid nitrogen cooled charged coupled device (CCD, Roper Scientific) camera [40, 41]. Light is delivered to tissue with a single source fiber and diffuse light is collected using multiple detector fibers arranged in a linear array. The concentrations of deoxy-, oxy-hemoglobin (C_{Hb}, C_{HbO_2}) are extracted using multi-wavelength and multi-source/detector separation ($\rho = 1.2, 2.4, 3, 4$) information. A multi-wavelength fitting algorithm was applied to directly extract C_{Hb}, C_{HbO_2} assuming absorption is coming from oxy- and deoxy- hemoglobin, $\mu_a = \sum_i \varepsilon_i C_i$ $(i = Hb, HbO_2)$. Here ε is the extinction coefficient of a given chromophore at a given wavelength obtained from literature [42]. It is also assumed that scattering parameter follows the Mie-type behavior in NIR spectral window, $\mu_s' = A\lambda^{-B}$. Here A and B are related to scatterer size and concentration and they were also fitted in the multi-wavelength fitting algorithm. After obtaining the hemoglobin concentrations, one can derive tissue oxygen saturation (StO_2) as $StO_2 = [C_{HbO_2}/(C_{HbO_2} + C_{Hb})] \cdot 100$.

2.5. *Statistical analysis*

All measured values are presented as the mean $\pm$ standard error (SE). Percent changes were determined individually for each mouse, based on pretreatment values. Statistical analyses were performed using Matlab (Mathwork, Inc.). Paired comparisons were performed by using Wilcoxon rank sum test to identify trends and substantial changes. Differences were considered significant for $p \leq 0.05$.

3. Results

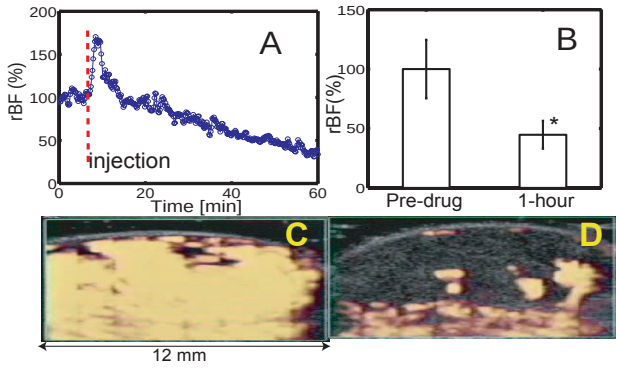

Fig. 1. (A) A representative DCS recording from a single animal showing the acute effects of the drug (in percent units with 100% implying no change).(B) DCS mean percent change in relative flow for $N = 9$ mice. (C) Effects of antivascular drug on tumor vasculature, imaged with micro-bubble contrast enhanced power Doppler ultrasound. In ultrasound images, yellow regions occur due to contrast enhancement in perfused blood vessels. Pretreatment tumor is uniformly perfused; (D) post treatment vasculature is destroyed, and blood perfusion is reduced. $\star$ denotes $p < .05$, when compared to baseline value.

#87255 - $15.00 USD Received 6 Sep 2007; revised 26 Oct 2007; accepted 29 Oct 2007; published 8 Nov 2007

3.1. *Combretastatin induces significant blood flow Reduction*

A representative example of DCS blood flow kinetics is shown in Figure 1(A). The data represent the single animal bulk tumor response averaged over multiple source-detector pairs before drug injection (baseline) and up to 1 hour after drug injection. The data are presented in percent units with 100% implying no change. It is clearly seen that blood flow decreased substantially following a transient initial flow increase. After 1 hour an $\sim$60% decrease in blood flow was observed. Figure 1(B) summarizes the average response of 9 such mice measurements, i.e. pre-drug (baseline) and 1 hour after drug injection. The average decrease in blood flow after 1 hour is $65 \pm 12\%$ $(p < 0.001)$.

Power Doppler ultrasound images of the same tumor (Fig. 1(C), (D)) show the effects of CA4P on vasculature. Yellow pixels denote perfused blood vessels of the tumor. It is clear that K1735 tumors were uniformly perfused with no evidence of avascular regions, suggesting that blood vessel growth kept up with tumor growth [29] (Fig. 1(C)). After injection of the drug, much of the vasculature was destroyed and blood perfusion reduced (Fig. 1(D)). Histological examination of tumor sections also reveals the blood flow reduction; luminal thrombi and occluded blood vessels were seen after 5 hours in addition to the presence of intraluminal collection of packed red blood cells or "blood cell lakes" (Fig. 2).

The biological reason for an initial increase in tumor blood flow during the first 10 minutes is not well understood. This effect, however, was observed consistently across all mice. Perhaps this early increase is due to an increase in heart rate induced by stress during drug injection. Moreover, it has been reported that the induction of anesthesia can induce 10 to 20 minutes physiological perturbation [29].

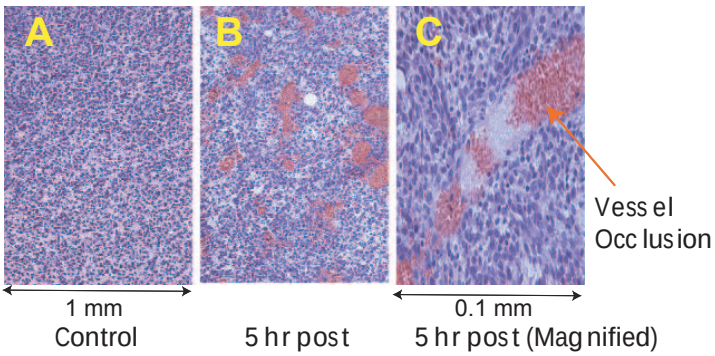

Fig. 2. Histology showing untreated (control) and CA4P-treated tumor sections. (A) Untreated tumor, dark blue spots represent tumor cell nuclei. (B) 5 hours post-treatment, red spots represent red blood cells. (C) 10 times magnified version of (B). It is clearly seen that after treatment, vessel occlusion occurs, blood vessels become congested and cells coagulated, forming "blood cell lakes" (B and C).

3.2. *Combretastatin induces significant blood oxygen saturation reduction*

The changes of blood flow (rBF) were accompanied by changes in blood oxygen saturation (StO_2). Our data from 5 mice show that mean blood oxygen saturation decreased significantly ($p < 0.005$) after one hour (Fig. 3(A)) from $47 \pm 7\%$ to $29 \pm 7\%$. Control mice showed no EF5 binding [31] (Fig. 3(B)), but substantial binding (shown in red) was found in treated tumors, again confirming that hypoxia is induced by the drug (Fig. 3(C)). These data demonstrate good correlation between intravascular oxygen status and intracellular oxygenation in this tumor

#87255 - $15.00 USD Received 6 Sep 2007; revised 26 Oct 2007; accepted 29 Oct 2007; published 8 Nov 2007

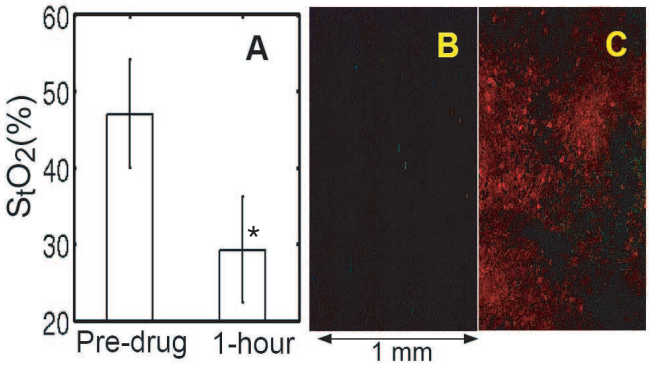

Fig. 3. (A) Mean percent change in StO_2 ($N = 5$). (B) EF5 immunofluorescence shows no binding for the control mice, but binding (shown in red) in the treated tumors showing hypoxia is induced (C). $\star$ denotes $p < .05$, when compared to baseline value.

model.

3.3. Radiation induced significant blood flow reduction

Figure 4(A) shows average blood flow for radiated mice ($N = 8$) before radiation, 7-days after and 14 -days after radiation. Irradiated K1735 tumors after 7 days were not statistically different ($p \geq 0.05$), but a clear decrease in blood flow was observed after 14 days ($p < 0.005$). The control group did not exhibit a statistically significant trend ($p \geq 0.05$). In total, these data demonstrate radiation induced vascular destruction and blood flow reduction in 14 days.

3.4. Radiation decreased blood oxygen saturation

Radiation treated and control groups did not exhibit significant changes in tissue blood oxygen saturation (StO_2) within 7 days ($p \geq 0.05$). However, evidently the significant blood flow fall-off produced a significant average StO_2 reduction ($p < 0.005, N = 8$) 14 days post radiation as shown in Figure 4(B). StO_2 variation in the control group was not statistically significant ($p \geq 0.05$). These observations are consistent with a previous study of EF5 binding that demonstrated tumor hypoxia was induced in treated mice after 2 weeks in the same tumor types [43].

4. Discussion

In this study, we examined the effects of antivascular and radiation therapies on tumor hemodynamics using a murine tumor model. K1735 melanoma tumors are well-suited for these studies since initially these tumors are well perfused and well oxygenated [29, 43]. Ultrasound Doppler micro-bubble injection confirmed K1735 tumors have relatively homogeneous vascularity throughout the whole tumor with very few regions of necrosis. Both the antivascular agent CA4P and radiation therapy induced vascular destruction, causing reduced blood flow and tissue oxygenation, and creating more regions of inefficient blood perfusion and hypoxia. The CA4P hemodynamic response was acute: Blood flow was reduced approximately 65% within the hour and tissue oxygenation was concurrently reduced by $\sim 38\%$.

Blood flow reduction due to CA4P has also been observed by other modalities. A study using superficial laser Doppler measurements showed a 73% decrease in tumor perfusion after 1 hour in a CH3 mouse mammary carcinoma model [44]. Dynamic contrast-enhanced magnetic resonance imaging (DCE-MRI) [45] and Doppler ultrasound [46] showed significant blood

#87255 - $15.00 USD Received 6 Sep 2007; revised 26 Oct 2007; accepted 29 Oct 2007; published 8 Nov 2007

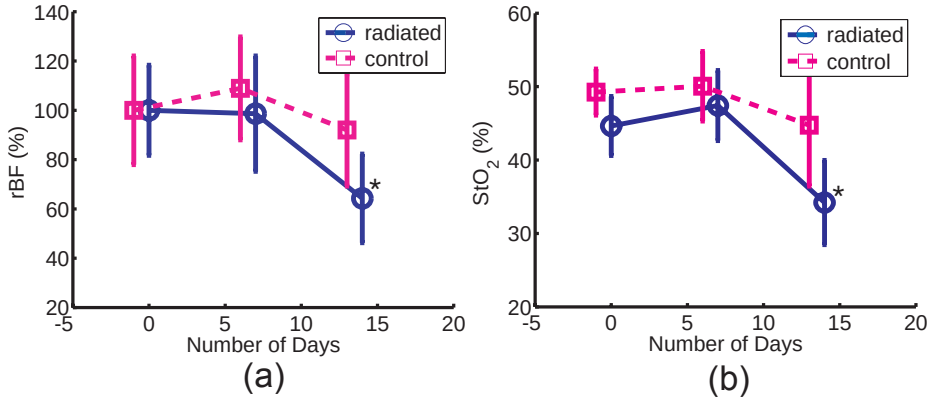

Fig. 4. (A) Average values of weekly *rBF* for both radiation treated mice and control groups ($N = 8$). Blood flow is normalized to initial (before radiation) value. $\star$ denotes $p < .05$, when compared to baseline value. (B) Average values of weekly StO_2 for both radiation treated mice and control groups ($N = 8$). $\star$ denotes $p < .05$, when compared to baseline value.

flow decrease in mice with human malignant melanoma (MeWo) tumor cell lines. Moreover, Phase I/II clinical trials of CA4P showed significant tumor anti-vascularity after the injection of tolerable doses. DCE-MRI detected reduced flow rate (37%, N=16) in recent clinical trials of different types of advanced solid tumor patients [47, 48] and PET observed a significant reduction in absolute blood flow (49%, N=13) by measuring tumor uptake of oxygen-15 (^{15}O)-labeled water in patients with advanced solid tumors [48, 49].

Compared to CA4P, radiation effects were more longitudinal: a single dose of radiation (12 Gy) induced a significant decrease in blood flow (36%, N=8) and oxygenation (24%, N=8) 2-weeks-post-radiation, but did not significantly modify these hemodynamic parameters 1-week-post-radiation. Moreover, it was previously observed in a similar study that 12 Gy of radiation retarded K1735 tumor growth and induced thrombosis, hemorrhage and hypoxia 2-weeks-post-radiation [43].

The average penetration depth of diffused photons in tissue is approximately one-third to one-half of the source-detector separation; thus our signal originates from $\sim$1-3 mm depth below the tissue surface. In clinical applications, sometimes as much as 2 - 3 cm depth of penetration has been achieved [19, 27]. We have initiated chemo-radiation therapy monitoring of head and neck cancer patients with superficial neck nodes [20] and chemotherapy monitoring of breast cancer patients [22]. These preliminary investigations suggest diffuse-optics-based therapy monitoring is feasible and may have clinical promise.

Diffuse optical techniques have unique advantages compared to other imaging modalities (e.g. MRI, PET and ultrasound), including low-cost, non-invasiveness and small size. Moreover, there has been significant recent interest in using antivascular therapy as an adjuvant to radiation therapy in order to develop more effective cancer therapies. The diffuse optical methods may play an important role in assessing acute and delayed responses in such newly developing combined therapy strategies.

#87255 - $15.00 USD Received 6 Sep 2007; revised 26 Oct 2007; accepted 29 Oct 2007; published 8 Nov 2007

5. Conclusion

In this work we have shown that tumor responses to an antivascular drug, CA4P, and to radiation can be assessed by noninvasively using diffuse optical spectroscopies in a pre-clinical mouse model. Although the temporal responses to CA4P and radiation were quite different, both CA4P and radiation were measured to induce significant blood flow and oxygenation reduction. The combined blood flow and blood oxygen saturation information may be valuable for understanding and assessing the working mechanism of antivascular drugs and radiation in both pre-clinical studies and clinical trials. Eventually, diffuse optical methods hold potential for evaluation of drug efficacy and prognosis of concurrent radiation and antivascular therapy. Such experiments should be a next step.

Acknowledgements

This research is supported by National Institutes of Health grants U54CA-105008-01 (W.M.F. Lee) and CA-87971 (A.G. Yodh). We are grateful to Dr. Cameron Koch for providing the EF5 reagents. The authors thank Dr. Theresa M. Busch for allowing us to use some of her lab facilities. Finally, we thank OXiGENE (Waltham, MA) for providing combretastatin A4-phosphate. U. Sunar's email address is sunar@sas.upenn.edu.

#87255 - $15.00 USD Received 6 Sep 2007; revised 26 Oct 2007; accepted 29 Oct 2007; published 8 Nov 2007